Anti-Swing Control of Suspended Loads on Shipboard Robotic Cranes

Jackrit Suthakorn
Department of Mechanical Engineering
Mahidol University, Salaya Campus
Bangkok 73170 Thailand
egjst@mahidol.ac.th

and

Gordon G. Parker
Department of Mechanical Engineering and Engineering Mechanics
Michigan Technological University
Houghton, MI 49931 USA
ggparker@mtu.edu

ABSTRACT

Currently, the speed at which materials can be transferred between ships at sea is limited by sea conditions. Rough sea conditions cause the payload to swing making load transfer difficult and time-consuming. The objective of this research is to develop a real-time, command compensating control for reducing sea state induced payload swing for shipboard robotic cranes. The future use of this control strategy will be to facilitate faster "ship-to-ship" payload transfer in rough sea conditions. In this study, only the sea-induced rotational motion of the ship is considered, since it is assumed that a station-keeping control maintains a constant position of the ship. This rotational motion is modelled using pitch-yaw-roll Euler angles. The shipboard robotic crane is modelled as a spherical pendulum attached to a three-degree-of-freedom manipulator. The three degrees-of-freedom are azimuth (rotation about an axis normal to the ship's deck), elevation (rotation about an axis parallel with the ship's deck, also referred to as luffing), and lift-line length. An inverse kinematics based approach and a sliding mode control strategy are explored. Both approaches use the azimuth and the elevation capability of the crane manipulator to maintain a horizontal position of the suspended load to reduce sea-induced payload sway.

KEYWORDS: shipboard crane controls, offshore construction, inverse kinematics, sliding mode control strategy.

1. INTRODUCTION

1.1 Overview

Currently, speed at which materials can be transferred from a transport ship to an offshore construction site is limited by sea conditions. Rough sea conditions cause the payload to sway making load transfer difficult and time-consuming. Figure 1 illustrates the application. The goal of this research is to develop a real-time, command compensating control for reducing sea state induced payload sway for shipboard cranes. In the future, this control strategy may facilitate faster ship-to-offshore payload transfer in rough sea conditions. In this study, the sea-induced rotational motion of the ship is considered, since it is assumed that a station-keeping control maintains a constant position (X_I, Y_I, Z_I) of the ship. This rotational motion is modeled using pitch-yaw-roll Euler angles (γ, η, δ). The shipboard crane is modeled as a spherical pendulum attached to a three-degree-of-freedom robotic manipulator. The three degrees-of-freedom are azimuth (rotation about an axis normal to the ship's deck), elevation (rotation about an axis parallel with the ship's deck, also referred to as luffing), and lift-line length. An inverse kinematics based approach and a sliding mode control strategy are explored. Both approaches use the azimuth and the elevation capability of the crane to maintain a horizontal position of the suspended load to reduce sea-reduced payload sway.

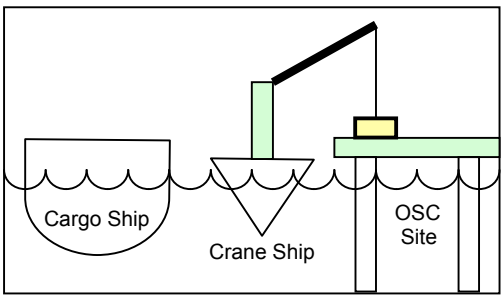

Figure 1: Ship Application.

Several studies focusing on shipboard crane control were previously explored. Examples of previous works are discussed here. McCormick and Witz investigated the parametric excitation of suspended loads during crane vessel operations [1]. In 1979, Yumori presented results of ocean testing of the Remote Unmanned Work System (RUWS) [2]. Yumori described his testing of the Motion Compensating Deck Handling System (MCDHS), using a feedback control system to minimize acceleration at the boom tip. Yumori used a real-time FFT cross-spectral analyzer to determine the dynamic

frequency characteristic of the MCDHS and the tether cable.

Vaha, Pieska and Timonen presented another application of payload sway control on offshore container cranes [3]. They applied an interactive task-level control for container handling where the task description used a laser pointing system, in conjunction with an optimal control system. Parker and Robinett introduced a successful strategy for eliminating sea disturbance induced payload sway for a 2-dimentional shipboard crane [4]. An inverse kinematics based approach, which uses the elevation capability of the crane to maintain a horizontal position of the suspended load was developed and shown to attenuate sway using a time domain simulation.

1.2 Control System and Simulation Architecture

In this study, a simulation model is constructed to simulate the control system. The simulation structure consists of a sway dynamics model , a sway cancellation model , a crane servo dynamics model, and operator command input and a sea disturbance input. The sway dynamics model implements the dynamic equations of motion of the payload in response to both ship and operator command inputs. The sway cancellation block receives the sea disturbance input and the payload states and generates the sway cancellation command input to the crane manipulator. When sea-induced payload sway occurs, the control system will command the crane manipulator to reduce the sway. The simulation architecture is show in the Figure 2.

2. SHIP/CRANE MODELING

In this section the dynamic equations of motion are developed in stages. In all formulations, Lagrange's equations are employed.

2.1 Stationary Crane

A diagram of the crane configuration used in this research is shown in Figure 3. This crane consists of the crane pedestal, boom, hoist-line, and payload. The constant height of the crane pedestal is denoted by *h*, the constant boom length is denoted by L_T, and the adjustable hoist-line length is denoted L_L. The inertial frame {I} has its origin at the ship's center of gravity, C.G. with positive Z_I axis vertical with respect to gravity and the X_I axis is along the ship's longest dimension. The {P} frame is attached to the pedestal, which rotates α about the positive Z_I axis. The vector from the ship's C.G. to the origin of the {1} frame components P_X, P_Y, and P_Z were represented in the {S} frame. The {1} frame is attached to the boom, which rotates β about $-Y_P$ axis. The {2} frame has its origin at the end of the boom, at the lift-line attachment point. The Z_2 axis is always aligned with X_P. The {3} frame has its origin coincident with the {2} frame with the $-Z_3$ axis along the lift-line. The {3} frame's orientation, relative to the {2} frame, is defined by two fixed angle rotations, which are the sway degrees-of-freedom as shown in Figure 4. Specifically, the radial sway is a rotation about the $-Y_2$ axis. The angle of the radial sway is called "theta", θ. The tangent sway is a rotation about the X_2 axis. The angle of the radial sway is called "phi", ϕ.

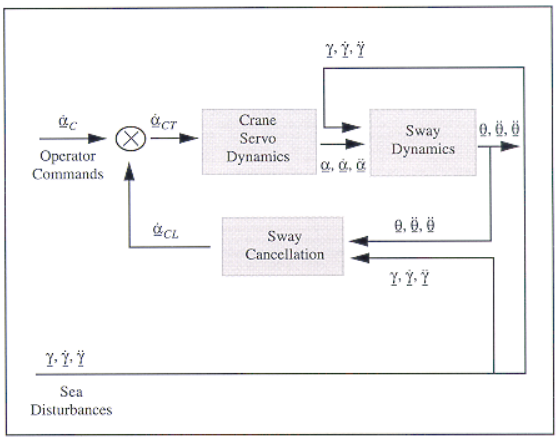

Figure 2: Simulation Architecture

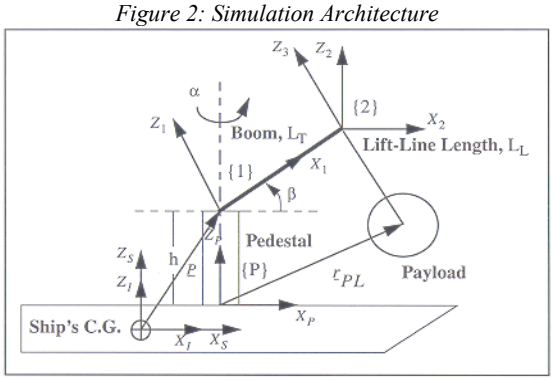

Figure 3: Stationary Crane.

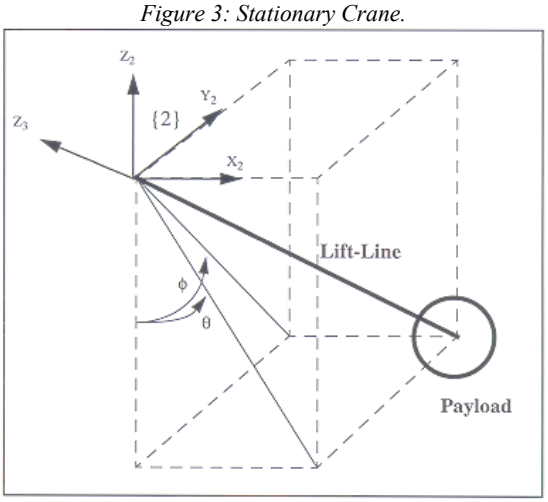

Figure 4: Payload and Lift-line.

The rotation matrix from the {S} frame to the {I} frame is the identity matrix

$$ {}^{I}_{S}R = I . $$

The rotation matrix from the {P} to the {S} frame is

$$ {}^{P}_{S}R = R_Z(\alpha) $$

capturing the crane's pedestal rotation capability. The rotation matrix from the {1} to the {P} frame is

$$ {}^{P}_{1}R = R_Y(\beta) $$

capturing the crane's luffing degree-of-freedom. The rotation matrix from the {2} frame to the {I} frame is

$$ {}^{I}_{2}R = R_Z(\alpha). $$

The rotation matrix from the {3} frame to the {2} frame is found according to the two fixed angle rotations as

$$ {}^{2}_{3}R = R_{-Y}(\theta) \cdot R_X(\phi). $$

The payload is assumed to be a point mass and acts as a spherical pendulum.

2.2 Payload Sway Equations for a Boom Crane on a Pitching Ship

A shipboard crane model on a pitching ship is modeled by mounting the stationary crane from Subsection 2.1 on a pitching ship. The pitching ship shown in Figure 5, uses frame {I} as the inertial frame. The {I} frame has its origin at the ship's C.G. Ship pitch is the angle γ measured from the X_I to the X_S axis The transformation matrix of the yawing motion from frame {S} to {I} can be described as:

$$ {}^{I}_{S}R = R_Y(\gamma) $$

and is the only change in defining ${}^{I}\vec{r}_{PL}$ as compared to the previous case.

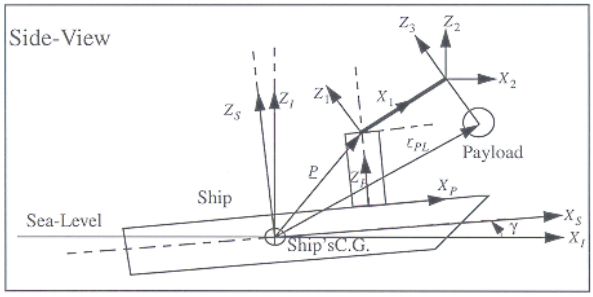

Figure 5: Pitching ship motion.

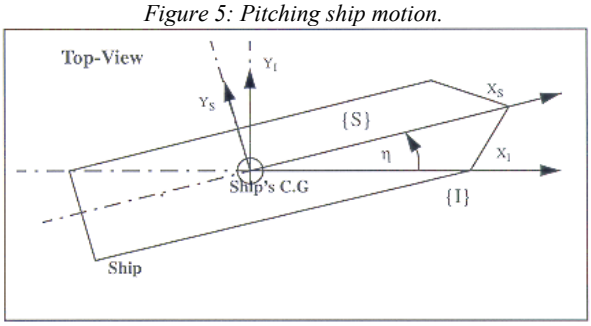

Figure 6: Yawing ship motion.

2.3 Payload Sway Equations for a Boom Crane on a Yawing Ship

A shipboard crane model on a yawing ship is modeled similar to the crane in the pitching ship. The rotational motion in the yawing ship is the rotation of frame {S}, which is attached to the ship, to the inertial, {I} frame. The yawing motion rotates about the Z_I axis by an angle named "eta", η. The transformation matrix of the yawing motion from frame {S} to {I} can be described as:

$$ {}^{I}_{S}R = R_Z(\eta). $$

The yawing ship model is shown as in Figure 6.

2.4 Payload Sway Equations for a Boom Crane on a Pitch + Yaw Ship

In this subsection, the shipboard crane model is modeled as in the last subsection. The rotational motion of the ship combines the pitching and yawing motion with the Pitch-Yaw Euler representation. The transformation matrix of the pitching + yawing motion from frame {S} to {I} can be described as:

$$ {}^{I}_{S}R = R_Y(\gamma)R_Z(\eta). $$

2.5 Equations of Motion

Equations of motion for each case can be determined by using Lagrange's equations:

$$ \frac{d}{dt}\left(\frac{\partial L}{\partial \dot{q}_i}\right) - \frac{\partial L}{\partial q_i} = 0, \qquad (1) $$

where $i = 1,2$

with $q_1 = \theta$ and $q_2 = \phi$ are applied to this system (see Figure 4) where the Lagrangian L

$$ L = T - V $$

Is the difference between the kinetic energy T and the potential energy V where

$$ T = \frac{1}{2} m_P ({}^{I}\dot{\vec{r}}_{PL})^T ({}^{I}\dot{\vec{r}}_{PL}) $$

and is the vector from the origin of the inertial frame {I} to the payload as shown in Figure 3, and m_P is the mass of the payload. The vector ${}^{I}\vec{r}_{PL}$ will be expressed in inertial coordinates, thereby ${}^{I}\dot{\vec{r}}_{PL}$ can be computed by simply forming the time derivative of its orthogonal components. The payload position vector is

$$ {}^{I}\vec{r}_{PL} = {}^{I}_{S}R({}^{S}\vec{P} + {}^{S}_{P}R\,{}^{P}_{1}R\,{}^{1}\vec{L}_T + {}^{S}_{2}R\,{}^{2}_{3}R\,{}^{3}\vec{L}_L) $$

where

$$ {}^{S}\vec{P} = \begin{bmatrix} P_X \\ P_Y \\ P_Z \end{bmatrix}, \; {}^{1}\vec{L}_T = \begin{bmatrix} L_T \\ 0 \\ 0 \end{bmatrix}, \; {}^{3}\vec{L}_L = \begin{bmatrix} 0 \\ 0 \\ -L_L \end{bmatrix}. $$

The dynamic equation of motion are generated automatically using the MAPLE symbolic manipulation program. Full details of the equations of motion for each case can be found in [5].

2.6 Sea Modeling

In this study, the sea models are simulated as sinusoidal. The sea disturbances are separated into two components. The first sea disturbance causes the rotational motion of the ship in pitch motion. The other one causes the rotational motion of the ship in yaw motion. Te

amplitude of the sine waves is 10 degrees, and the frequency of this sine wave is 0.1 Hz.

3. CONTROL FORMULATIONS

In this section, an inverse kinematics sway cancellation control strategy is discussed. Due to limitations of the inverse kinematics approach for general crane configurations, a nonlinear control strategy is employed. To this end an application of Lyapunov's direct method and sliding mode control to the sway control problem is presented.

3.1 Inverse Kinematics Based Approach

The objective of the sway cancellation control is to use the crane's actuation capability to keep the hoist-line vertical (with respect to gravity) thereby inhibiting the onset of swing. This is equivalent to setting $\theta, \phi = 0$. In addition, the constraint of keeping the horizontal position of the payload constant will be imposed. This allows positioning of the payload with respect to a fixed reference point.

The integration based inverse kinematics approach may be extended to the more complicated case of additional crane DOF and disturbances and is described in [Suthakorn 1998]. However, a potential limitation of the method is its lack of robustness. Specifically, there is no guarantee of stability if model errors are present. Therefore a sliding mode control approach will be pursued instead.

3.2 Active Sway Damping Sliding Mode Control

In an effort to express the dynamic equation and control law compactly, the following quantities are define:

- $\vec{\alpha}, \dot{\vec{\alpha}}, \ddot{\vec{\alpha}} \equiv$ vectors of the angles, rates, angular accelerations of crane manipulators (azimuth, $\alpha, \dot{\alpha}, \ddot{\alpha}$ and boom, $\beta, \dot{\beta}, \ddot{\beta}$)
- $\vec{\theta}, \dot{\vec{\theta}}, \ddot{\vec{\theta}} \equiv$ vectors of the sway angles, rates of sways, angular accelerations of sways (radial sway, $\theta, \dot{\theta}, \ddot{\theta}$ and tangent sway, $\phi, \dot{\phi}, \ddot{\phi}$)
- $\vec{S} \equiv$ a vector of the sliding surface.
- $\vec{V} \equiv$ a vector of controller design parameters used to achieve robustness.
- $w \equiv$ a matrix of control design gains used to set the sway time constant.
- $a \equiv$ a matrix of the coefficients of the angular accelerations of crane's DOF.

Using this notation the sway equations of motion in Equation (1) can be written in a compact form as

$$\ddot{\vec{\theta}} + \vec{V} + a\ddot{\vec{\alpha}} = 0 \qquad (2).$$

The desired sway dynamics are defined by the sliding surface as

$$\vec{S} = \dot{\vec{\theta}} + w\vec{\theta} \qquad (3)$$

and

$$\dot{\vec{S}} = \ddot{\vec{\theta}} + w\dot{\vec{\theta}} \qquad (4)$$

Where $w = \begin{bmatrix} w_1 & 0 \\ 0 & w_2 \end{bmatrix}, \vec{S} = \begin{bmatrix} S_1 \\ S_2 \end{bmatrix}, \dot{\vec{S}} = \begin{bmatrix} \dot{S}_1 \\ \dot{S}_2 \end{bmatrix}$.

Substituting Equation (1) into Equations (3) and (4) gives

$$-V - a\ddot{\vec{\alpha}} + w\dot{\vec{\theta}} = 0 \qquad (5).$$

Next, the crane inputs are solved as

$$\ddot{\vec{\alpha}} = a^{-1}[-\vec{V} + w\dot{\theta}] \qquad (6).$$

The final law is formed by appending the typical term, discontinuous in $\vec{S}$, it the control law of Equation (6).

$$\ddot{\vec{\alpha}} = a^{-1}[-\vec{V} + w\dot{\theta} - A\,\mathrm{sgn}(\vec{S})] \qquad (7)$$

Where

$$A = \begin{bmatrix} A_1 & 0 \\ 0 & A_2 \end{bmatrix}$$

The crane boom and azimuth rates are obtained by integrating Equation (7) once. Stability of the closed-loop system is demonstrated using Lyapunov's direct method. A Lyapunov candidate function is selected as

$$\vec{Z} = \frac{1}{2}\vec{S}^T\vec{S} \qquad (8).$$

For the system to be stable, it must be shown that $\dot{\vec{Z}} < 0$. Taking the time derivative of $\vec{Z}$

$$\dot{\vec{Z}} = \vec{S}^T\dot{\vec{S}} \qquad (9)$$

substitute Equation (9) from Equations (3), (4), (5), and (7):

$$\dot{\vec{Z}} = \vec{S}^T[\ddot{\vec{\theta}} + w\dot{\vec{\theta}}] \qquad (10.1)$$

$$= \vec{S}^T[-V - a\ddot{\vec{\alpha}} + w\dot{\vec{\theta}}] \qquad (10.2)$$

$$= \vec{S}^T[-w\dot{\theta} + A\,\mathrm{sgn}(\vec{S}) + w\dot{\vec{\theta}}] \qquad (10.3)$$

$$= \vec{S}^T[A\,\mathrm{sgn}(\vec{S})] \qquad (10.4).$$

From Equation (10), if the diagonal elements of *A* are negative then $\dot{\vec{Z}}$ is less than zero. Based on Lyapunov's Direct Method, this shows that the system is asymptotically stable when:

$$\vec{u} = -\vec{V} - \vec{a}\ddot{\vec{\alpha}} \qquad (11.1)$$

and

$$\vec{u} = -w\dot{\vec{\theta}} - A\,\mathrm{sgn}(\vec{S}) \qquad (11.2)$$

then,

$$\ddot{\vec{\alpha}} = a^{-1}[-\vec{V} + w\dot{\vec{\theta}} - A\,\mathrm{sgn}(\vec{S})] \qquad (12).$$

Equation (12) is used in the swing feedback approach to solve the swing cancellation in an inverse kinematics approach.

4. SIMULATION RESULTS

This section examines three types of crane systems: pitch-only, yaw-only, and pitch-yaw. The differences of each case are the sea disturbances inducing the

rotational motion of the ship. The sea disturbance is modeled as sinusoid. A MATLAB SIMULINK time domain simulation was constructed to assess of the control system. It uses two CMEX S-FUNCTION blocks to implement the computationally intensive dynamic state update equations. These files must be compiled before using the simulation. In all the test cases, the crane has an initial boom angle of 45 degrees, a boom length of 10.0m, and a pedestal height of 1.0m. The length between the base of the crane and the C.G. of the ship is 0.5m. The lift-line length is 6.2m and held fixed, yielding a nominal pendulation frequency of 0.2 Hz. The payload is assumed to be a point mass of 1.0kg. The amplitude of the sea-disturbances was chosen as 10 degrees, and their frequencies as 0.1 Hz. The pitch disturbance starts at $t=1$ second and the yaw disturbance starts at $t=10$ seconds. The results of this study are present in each case.

- **Pitch-Only System**

In the pitch-only system, only radial sway will occur. Therefore, only the boom motion is used to eliminate the sway. The boom angle and azimuth angle responses are shown in Figures 7(a) and (b). Although the boom angle shows a drifting of its average value, it is much less than without the simulated operation-in-the-loop. Sway-cancellation on and off plots are shown in Figures 8(a) and (b), indicating a 6 dB reduction in sway magnitude.

- **Yaw-Only System**

Although the ship experiences only a yaw disturbance, both radial and tangent sway have the potential to be excited. However, this analysis assumed that pitch, yaw, and roll angles are very small. Because of this assumption, the centripetal acceleration terms are zero. Since it is those disturbance terms which excite radial sway, there is no radial sway in this case excited by the disturbance. However, the azimuth angles are not assumed small. Therefore, the control action of the crane's pedestal does excite radial sway which is compensated by the control system. The four plots of boom, azimuth, radial and tangential sway are shown in Figures 9(a), 9(b), 10(a), and 10(b). The tangential sway is reduced by 20 dB. However, the azimuth motion, due to the control system, causes radial sway. The boom control system engages to damp the radial sway.

- **Pitch-Yaw System**

In this case, pitch and yaw ship motion induces sway in both radial and tangential directions. The four plots of boom, azimuth, radial and tangential sway are shown in Figures 11(a), 11(b), 12(a), and 12(b). For this case, the amplitude of both radial sway and tangent sway are reduced by about 20 dB.

Additional case studies (1. different disturbance amplitudes, 2. different disturbance frequencies, and 3. same disturbance starting time) were also performed. The results shown that this control system can successfully reduce the swing of the suspended load in these cases. Full details of the additional case studies can be found in [5].

5. CONCLUSION AND FUTURE WORK

5.1 Conclusion

A methodology and results of the analysis and control design on the topic of anti-swing of suspended loads on shipboard cranes was presented. Inverse kinematics and sliding mode control approaches were developed for sway control of multiple degree of freedom cranes. The sliding mode control was selected for final simulation evaluation due to its stability. The simulation results indicated the ability to eliminate payload swing in pitch-only, yaw-only, and pitch-yaw systems. The use of an inverse kinematics and sliding mode control approach on shipboard cranes, which have boom and azimuth capability, is effective.

5.2 Recommendations for Future Work

- Sea modeling: The sea model in this study was simulated using a sine wave. To eliminate realistic sea disturbance induced payload swing on shipboard cranes, a more realistic sea model is required. The "Simulation Time History Computer Program," available from the U.S. Department of Defense, providing random wave time histories of 6 DOF ship response, could be used.
- Investigating other crane configurations to actively damp swing for the full roll-pitch-yaw system.
- Investigation of the combined effects of operator command and sea-disturbance on payload swing. In addition, the development of coordinated payload swing control systems through simulation and operator-in-the-loop testing.

6. REFERENCES

[1] McCormick, F.J., Witz, J.A., 1993, *An Investigation into Parametric Excitation of Suspended Loads During Crane Vessel Operations*. Underwater Technology, pp. 30-39.

[2] Yumori, I.R., 1979, *Ocean Testing of Motion Compensating Crane and Kevlar Tether Cable Dynamics for an Unmanned Deep Submersible Using Real Time Spectral Analysis*, Ocean Ann. Conf. of IEEE (Oceaning Engr.) and Mar Tech. Soc., pp. 764-771.

[3] Vaha, P., Pieska, S., Timonen, E., 1988, *Robotization of an Offshore Container Crane*, Technical Research Center of Finland, pp. 637-648.

[4] Parker, G.G., Petterson, B., Dohrmann, C.R., Robinett, R.D., *Vibration Suppression of Fixed-Time Jib Crane Maneuvers*, Mar 1995, Proc. of SPIE – the Int'l Soc. of Optical Engr. Smart Struc. and Mat., Ind. and Comm. App. of Smart Struc. Tech., Vol. 2447, pp. 131-140.

[5] Suthakorn, J., *Anti-Sway Control of Suspended Loads on Shipboard Cranes*, 1998, MS Thesis, Dep.t of ME-EM, Michigan Tech University.

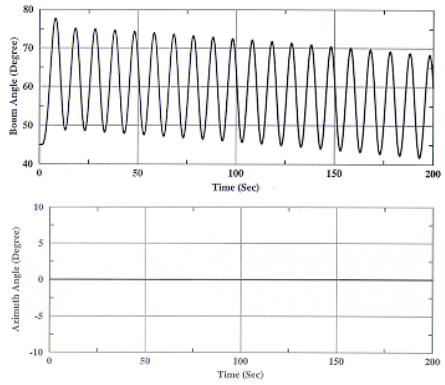

Figure 7(a): Boom angle, 7(b): Azimuth angle histories, when the controller is on/off for the pitch-only case.

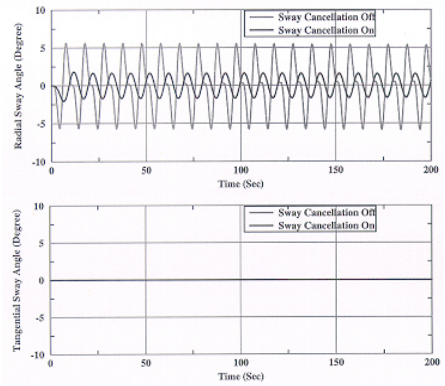

Figure 8(a): Radial sway angle, 8(b): Tangential sway angle histories with control on/off for the pitch-only case.

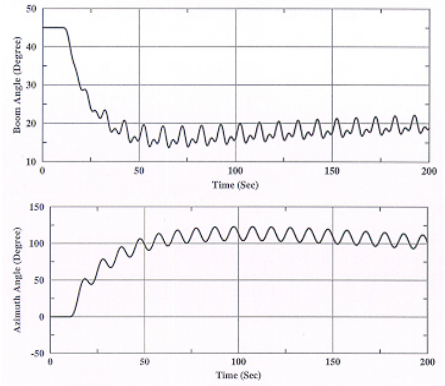

Figure 9(a): Boom angle, 9(b) Azimuth angle histories, when the controller is on/off for the yaw-only case.

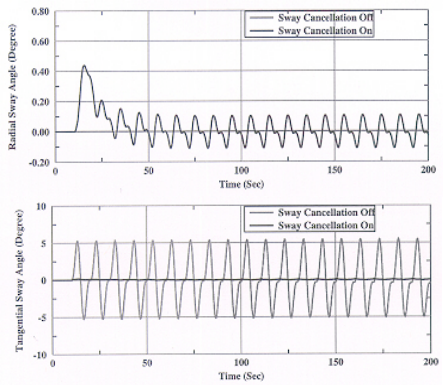

Figure 10(a): Radial sway angle, 10(b): Tangential sway angle histories, with control on/ off for the yaw-only case.

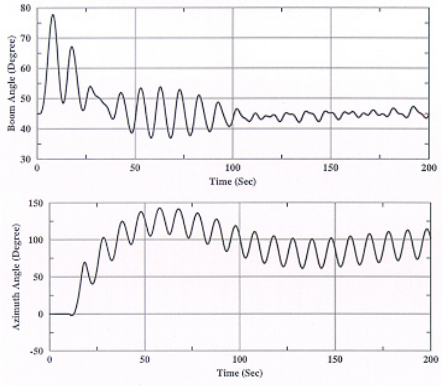

Figure 11(a): Boom angle, 11(b): Azimuth angle histories, when the controller is on/off for the pitch-yaw case.

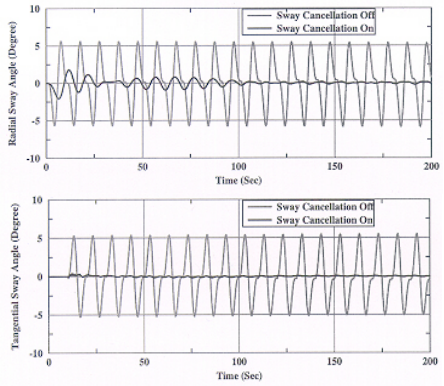

Figure 12(a): Radial sway angle history, 12(b): Tangential sway angle history, with control on and off for the pitch-yaw case